A Statistical Method for Comparing Chest Radiograph Images of MTB Patients

Norliza Mohd. Noor†, Omar Mohd. Rijal*, Shee Lee Teng*
†Diploma Program Studies, Universiti Teknologi Malaysia
* Institute of Mathematical Science, University Malaya
norliza@citycampus.utm.my , omarrija@um.edu.my, sheeleeteng@yahoo.co.uk

Abstract :- Digital images of chest radiograph taken at different time points may be compared to investigate the effect of treatment on mycobacterium tuberculosis (MTB) patients. One method of comparison is that of visually locating "snow-flakes" which should decrease in area or size with each subsequent image. This paper propose a more objective method; the comparison of image histograms whereby a leftward shift of the histogram indicates a positive effect of treatment. The comparison of two histograms is equivalent to either comparing the corresponding box-plots or the corresponding set of percentiles. However, before the comparison is made the images need to be registered and resized. The results of this study show that the proportion of percentiles (from histogram) can be used as an indicator of treatment effect (or patient's progress). Further the correlations R_F^2 is shown to be the best similarity measure to indicate the quality of image registration. Finally, this study also shows that a combination of registration and resizing can improve the pair-wise comparison.

Key Word:- Chest Radiograph, Mycobacterium Tuberculosis, Image Registration, Resizing, Correlations, Box-plot.

1 Introduction

Two million deaths are due to MTB [1] annually. Global TB incidence is still growing at 1% a year. To eliminate the problem of TB the WHO [1] makes several suggestions, in particular "Giving access to quality TB diagnosis and treatment for all". An important ingredient [2], [3], [4] for diagnosis of TB is the comparison of a series of chest X-rays. If treatment is successful, the presence of "snowflakes" will decrease or diminish with each subsequent (new) image. In other words it is important that we have a reliable method of comparing X-ray images.

Several problems have to be faced before any comparison may be made. Firstly, the diseased area or snowflakes do not subscribe to any fixed dimensions (shape, size, or orientation), [4]. As such two images may only be compared by their direct difference since no obvious feature may be considered. In particular if treatment is successful, the incidence of snowflakes shows a reduction in the second image. Any measure of this reduction will indicate success of treatment.

To measure the direct difference between images, the images must be registered [5], [6], [7]. In some cases the image may also have to be resized, see Fig. 1(a), Fig. 1(b) and Fig. 1(c).

In this study images at three time points will be considered; namely the first visit, second visit and the last visit. The various stages for comparison involve;

(i) Image registration using SCPR (see section2).
(ii) Cropping the lung area.
(iii) Resizing subset images from (ii), (see section3).
(iv) Selecting the region of interest that is the affected area indicated by the presence of snow-flakes (under expert advice [4]).
(v) Obtaining image histograms and hence box-plots of image in (iv).
(vi) Comparing box-plots or equivalently percentile from image histograms.

To ensure the quality of registration, similarity measure R_F^2 and R_S^2, MSE and PSNR will be used. Section 6 is a short study showing that R_F^2 is the best choice of similarity measures, which in turn is an appropriate indicator of quality registration..

In this study, let $\{I(i,j);\ i = 1, \ldots, M,\ j = 1, \ldots, N\}$ represent the digital X-ray image of a patient on his first visit to the hospital. Let $\{K(i,j);\ i = 1, \ldots, M,\ j = 1, \ldots, N\}$ represent the same patients image at a later prescribed time point.

(a) (b) (c)

Fig. 1 Three original images of the same patient taken at three different time points.
(a) 1st visit, image size: 2800×2048
(b) 2nd visit, image size: 2500×2048
(c) 3rd visit, image size: 2769×2048

2 Seven control point registration (SCPR)

Let $A = (x_A, y_A)$, $B = (x_B, y_B)$,..., $G = (x_G, y_G)$ be 7 selected points on the lung area. Given two images (two time points) we have,

1st image $\equiv \{A, B, C, D, ..., G\}$

2nd image $\equiv \{A', B', C', D', ..., G'\}$.

The following distances were calculated:

$$D_{AA'}, D_{BB'}, \ldots, D_{GG'}$$

where for example

$$D_{AA'} = \sqrt{(x_A - x_{A'})^2 + (y_A - y_{A'})^2}$$

Hence each pair of images were registered as follows; calculate,

$$T_{xA} = (x_A - x_{A'})$$
$$T_{xB} = (x_B - x_{B'})$$
$$\vdots$$
$$T_{xG} = (x_G - x_{G'})$$

and let $T_x = median\{T_{xA}, T_{xB}, \ldots, T_{xG}\}$.

Similarly calculate

$$T_{yA} = (y_A - y_{A'})$$
$$T_{yB} = (y_B - y_{B'})$$
$$\vdots$$
$$T_{yG} = (y_G - y_{G'})$$

and let $T_y = median\{T_{yA}, T_{yB}, \ldots, T_{yG}\}$.

Treating the 1st image as a reference image, then the 2nd and 3rd image were subject to a vertical displacement T_y and a horizontal displacement T_x.

The images are said to be properly registered if the distances $D_{AA'}, D_{BB'}, \ldots, D_{GG'}$ are reduced or minimized.

It can be shown (see Table 1) that $D_{AA'} = 143.8367$ (for 1st and 2nd image) whilst $D_{AA'} = 35$ after SCPR. Similar results hold for all other 7 points.

Table 1 Distance between 7 control points for SCPR for 1st and 2nd image given in Fig. 1.

	(Before translation) (1st and 2nd)	(After translation) (1st and 2nd)	(T_x, T_y)
$D_{AA'}$	143.8367	35	(-33,175)
$D_{BB'}$	175.2767	60.9262	
$D_{CC'}$	146.1677	49.4065	
$D_{DD'}$	194.0773	42.1900	
$D_{EE'}$	175.0457	37	
$D_{FF'}$	236.8122	61.4003	
$D_{GG'}$	222.0090	58.6003	

3 Resizing

A view of the original image shows that a significant area of the image is taken – up by the irrelevant background. Further Figure 1 shows that the three images are of different size, and this may have a significant effect on comparison of images.

This study proposes that the image be resized as follows;

A) The image is cropped such that the remaining image is essentially the lung area.

B) Then an affine transformation is carried out using the MATLAB command

$$\text{MAKETFORM ['affine', } \begin{pmatrix} C_x & 0 & 0 \\ 0 & C_y & 0 \\ 0 & 0 & 1 \end{pmatrix} \text{]}$$

where for example in Figure 1, $C_x = \frac{2500}{2800} \approx 0.9$. and $C_y = \frac{2048}{2048} = 1$. C_x and C_y is the required percentage for resizing. The program will then interpolate the new pixel value using the bilinear interpolation.

4 Brief Review of ULFR and R_F^2

Re-label the observations (or experimental values) of {$I(i,j)$; i = 1, …, M, j= 1, …, N} as $y_1, y_2, \ldots, y_{MN}$, the observations of {$K(i,j)$; i = 1, …, M, j= 1, …, N} as $x_1, x_2, \ldots, x_{MN}$, and the true $I(i,j)$ and $K(i,j)$ values will be denoted by $Y_1, Y_2, \ldots, Y_{MN}$ and $X_1, X_2, \ldots, X_{MN}$, respectively. We look at two regression models to study the relationship between y_i and x_i.

We first look at the ordinary simple linear regression (SL) model [8] of the dependent variable, y_i and explanatory variable, x_i:

$$y_i = \alpha_s + \beta_s x_i + \varepsilon_i, \quad i = 1, 2, \ldots, MN \qquad (1)$$

where the maximum likelihood estimators (MLE) and COD are given as follows:

$$\hat{\alpha}_s = \bar{y} - \hat{\beta}_s \bar{x}, \quad \hat{\beta}_s = \frac{S_{xy}}{S_{xx}}$$

and $$R_s^2 = \frac{\hat{\beta}_s S_{xy}}{S_{yy}} \qquad (2)$$

where the R_s^2 is the proportion of variation explained by explanatory variable x and

$$\bar{y} = \frac{\sum y_i}{MN}, \bar{x} = \frac{\sum x_i}{MN},$$
$$S_{yy} = \sum (y_i - \bar{y})^2,$$
$$S_{xx} = \sum (x_i - \bar{x})^2$$

and $$S_{xy} = \sum (x_i - \bar{x})(y_i - \bar{y}).$$

However, as pointed out by [9], the assumption that the explanatory variable can be measured exactly may not be realistic in many situations. The estimates of explanatory variable may contain measurement error arising from the techniques or instruments used or trying to quantify a variable that has no physical dimension. In these cases, the explanatory variable is subject to error.

Suppose that now the X and Y are two linearly related unobservable variables (see [10] and [11])

$$Y_i = \alpha + \beta X_i \qquad (3)$$

and the two corresponding random variables x and y are observed with error δ and ε respectively

$$\left.\begin{aligned} x_i &= X_i + \delta_i \\ y_i &= Y_i + \varepsilon_i \end{aligned}\right\} \quad i = 1, 2, \ldots, MN \qquad (4)$$

where δ_i and ε_i are mutually independent and normally distributed random variables. Equation (3) and (4) are known as the ULFR model when there is only one relationship between the two variables X and Y. It can be shown that the maximum likelihood estimators when the ratio of the error variances is equal to one, $\frac{\sigma_\varepsilon^2}{\sigma_\delta^2} = \lambda = 1$, are given as follows:

$$\hat{\alpha}_F = \bar{y} - \hat{\beta}_F \bar{x} \qquad (5)$$

$$\hat{\beta}_F = \frac{(S_{yy} - S_{xx}) + \{(S_{yy} - S_{xx})^2 + 4S_{xy}^2\}^{1/2}}{2S_{xy}} \qquad (6)$$

$$\hat{\sigma}_\delta^2 = \frac{1}{MN - 2}\left[\sum (x_i - \hat{X}_i)^2 + \frac{1}{\lambda}\sum (y_i - \hat{\alpha} - \hat{\beta}\hat{X}_i)^2\right] \qquad (7)$$

and $$\hat{X}_i = \frac{x_i + \hat{\beta}(y_i - \hat{\alpha})}{\lambda + \hat{\beta}^2} \qquad (8)$$

The equation in (3) and (4) can be written as

$$y_i = \alpha_F + \beta_F x_i + (\varepsilon_i - \beta_F \delta_i)$$
$$= \alpha_F + \beta_F x_i + V_i \quad \text{for } i = 1, \ldots, MN \qquad (9)$$

where the error of the model, V_i is normally distributed. The residual sum of squares and the regression sum of squares are given as follows:

$$S_E = \frac{S_{yy} - 2\hat{\beta}S_{xy} + \hat{\beta}^2 S_{xx}}{1 + \hat{\beta}^2}$$

and

$$S_R = S_{yy} - S_E$$
$$= S_{yy} - \frac{S_{yy} - 2\hat{\beta}S_{xy} + \hat{\beta}^2 S_{xx}}{1+\hat{\beta}^2}$$

Therefore, the COD for ULFR can be defined as

$$R_F^2 = \frac{S_R}{S_{yy}} = \frac{\hat{\beta}_F S_{xy}}{S_{yy}} \qquad (10)$$

and it can be shown that $0 \le R_s^2 \le R_F^2 \le 1$.

5 MSE and PSNR

Two other indicators of proper registrations are the MSE and PSNR defined as follows:

$$MSE = \frac{1}{mn}\sum_{i=0}^{m-1}\sum_{j=0}^{n-1} \| I(i,j) - K(i,j) \|^2$$

where *I* is second visit image and *K* is the first visit image,

and $$PSNR = 20 \times \log_{10}\left(\frac{MAX}{\sqrt{MSE}}\right)$$

where $MAX = 2^B - 1, \quad B = bit$. The digital image is coded using 12bit DICOM format, therefore $MAX = 2^{12} - 1 = 4095$.

6 Ability of Similarity Measures to Compare Images

Due to the complex dimensions of the snowflakes, an initial experiment simulates the situation where the same object (plaque shown in Fig. 2(a), Fig. 2(b) and Fig. 2(c)) is captured on camera at different distances. This is equivalent to the same patient at different distances or positions from the X-ray camera (possibly due to radiographer error).

Fig. 2 (d), Fig. 2(e) and Fig. 2(f) are the cropped image of Fig. 2(a), Fig. 2(b) and Fig. 2(c) respectively. These cropped images are equivalent to the corresponding lung area after removal of irrelevant background. To compare these cropped images, the image dimensions must be the same.

Clearly the images are not identical pixel-wise (pixel (i, j) image shown in Fig. 2(d) and pixel (i, j) image shown in Fig. 2(e)). Henceforth an indicator of image similarity is necessary.

Table 2 shows that R_F^2 is the best similarity measure (no resizing or registration). In this case R_F^2 is actually the best indicator of 'dissimilarity'.

Table 3 (after registration with 4 control points and resizing, see Fig. 3 and Fig. 4) again show that R_F^2 is a good indicator of similarity for the same images in Fig. 4(a), Fig. 4(b) and Fig. 4(c). However MSE and PSNR may also be used.

Since R_F^2 can indicate both similarity and dissimilarity between images, all future discussion will be confined to the use of R_F^2.

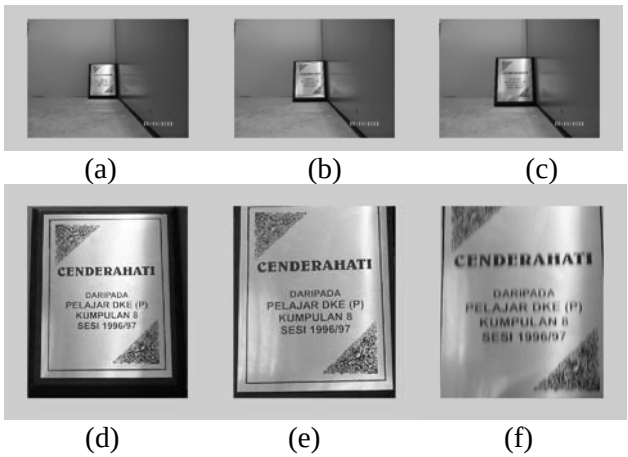

(a) (b) (c)

(d) (e) (f)

Fig. 2 One object taken at three different distance using the same camera that produce the same image size of 1944×2592, (a) Camera distance:72 cm, (b) Camera distance:62 cm, (c) Camera distance:52 cm. (d), (e) and (f) is the image of region of interest cropped with image size of 574×488.

(a) 574×488 (b) 675×563 (c) 808×683

Fig. 3 Sub image from Fig. 2 (a), Fig. 2(b) and Fig.2(c) respectively after 4 control point registration. Note the different image size though the region of interest is captured.

(a) (b) (c)

Fig. 4 The resultant image from Fig. 3 after resizing with Affine transformation. All images has the same size of 574×488 pixels.

Table 2 Comparison of similarity measures (No resizing and no translation)

Similarity measures	Images (Fig. 2)	
	(d)-(e)	(d)-(f)
R_F^2	0.1350	0.0499
R_S^2	0.0747	0.0376
MSE	8213.0	8093.2
PSNR	8.9858	9.0496

Table 3 Comparison of similarity measures (with 4 control points registration and Affine resizing method)

Similarity measures	Images (Fig. 4)	
	(a)-(b)	(a)-(c)
R_F^2	0.7191	0.7905
R_S^2	0.5592	0.6754
MSE	3103.7	2257.4
PSNR	13.2120	14.5947

7 Comparing Two Images

Since only a small section of the original image is to compared, the image histogram is a potential tool for comparison. However, a simpler way of comparing two distributions is in fact the comparison of two box-plot [12] or its corresponding percentiles. For clarity, the p^{th} percentile is defined to be that value of a variable for which p percent of the values of the distribution are smaller.

8 Descriptions of the Experiments

For each patient, his series of visits to the hospital and consequently the chest x-ray images obtained are labeled A, B and C. The minimum treatment period for MTB is 6 months and the progress is monitored every 2 months via clinical test (usually the sputum test) and chest x-ray images. In this study the chest x-ray images are compared pair-wise, for three time points, that is first and the second chest x-ray (AB), first and last chest x-ray (AC), see Fig. 5(a), Fig. 5 (b), Fig. 5 (c).

The X-ray films were scanned into 12 bit DICOM file using Kodak LS 75 X-ray film scanner.

The experiments were carried out as follows;

(a) The images were subjected to SCPR with the 1st visit image being the reference image (see Fig. 5(d), Fig. 5 (e), Fig. 5 (f)).
(b) The lung area was cropped as being the region of interest see Fig. 5(g), Fig. 5 (h), Fig. 5 (i).
(c) Resizing is carried out using Affine transformation. Resultant image is shown in Fig. 5(j), Fig. 5 (k), Fig. 5 (l).
(d) High density area of MTB is selected for comparison, Fig. 5(m), Fig. 5 (n), Fig. 5 (o).
(e) The corresponding box-plot for (d) was given in Fig. 6.

9 Results and Discussion

Section 6 has shown that R_F^2 is a good indicator of similarity (or dissimilarity) between a pair of digital images. Further, comparing R_F^2 values between Table 2 and Table 3 clearly show that after SCPR and resizing the pair of images may then be considered suitable for comparison (by direct difference).

Nineteen patients were studied and Fig. 5 illustrates the main stages of the experiments. The crucial result is given in Fig. 6 which show a left-ward shift of box-plot. Looking simultaneously at Fig. 6 and Fig. 5(m), Fig. 5(n), Fig. 5(o), clearly show that as the white area or snowflakes decrease in intensity, we observed the left-ward shift in the image histogram. In other words, Fig. 6 indicates that the patient is making a positive progress.

However, comparing histograms for large numbers of patients may prove to be inconvenient. As such eleven percentile (10, 20, 25, 30, 40, 50, 60, 70, 75, 80, 90) from the image histogram is calculated, and Table 4 shows the number (total) of percentile with the left-ward shift.

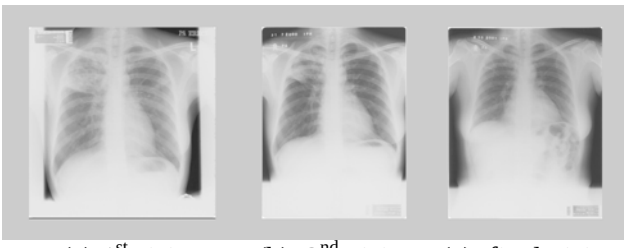

(a) 1st visit size: 2096 x 2048 (b) 2nd visit 2800 x 2048 (c) final visit 2548 x 2048

(d) 1st visit size: 2096 x 2048 (e) 2nd visit 2096 x 2048 (f) final visit 2096 x 2048

(g) 1st visit size: 1650 x 1486 (h) 2nd visit 1910 x 1852 (i) final visit 1564 x 1568

(j) 1st visit size: 1564 x 1468 (k) 2nd visit 1564 x 1468 (l) final visit 1564 x 1468

(m) 1st visit size: 352 x 644 (n) 2nd visit 352 x 644 (o) final visit 352 x 644

Fig. 5 Description of the experiment.
(a), (b), (c) Original image
(d), (e), (f) Resultant image after SCPR.
(g), (h), (i) Cropped out the region of interest
(j), (k), (l) Resized image using Affine Transformation
(m), (n), (o) Selected Area: High Density MTB Infected Area

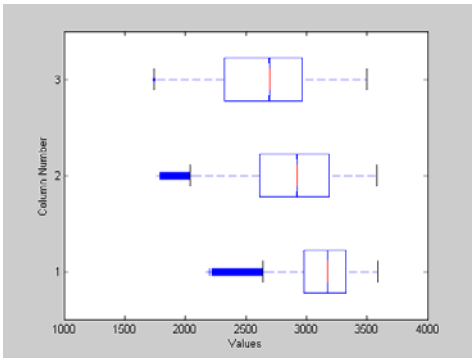

Fig. 6 Lowest box-plot corresponds to subset image from the 1st visit similarly top-most box-plot is for the last visit.

Table 4 Percentiles of 20 MTB patients.

Patients	1st visit and 2nd visit		1st and Last visit	
	(+)	(-)	(+)	(-)
1 (165500)	11	0	11	0
2 (93400)	11	0	7	4
3 (95600)	11	0	11	0
4 (110800)	0	11	0	11
5 (144400)	0	11	0	11
6 (148700)	0	11	0	11
7 (118600)	0	11	0	11
8 (94100)	4	7	4	7
9 (238300)	0	11	0	11
10 (234000)	0	11	0	11
11 (15701)	0	11	1	10
12 (55601)	0	11	0	11
13 (82601)	0	11	0	11
14 (299102)	0	11	0	11
15 (341402)	0	11	0	11
16 (384102)	0	11	0	11
17 (390002)	0	11	0	11
18 (392602)	5	6	0	11
19 (393202)	11	0	11	0

Fourteen patients showed clear-cut recovery with ten or eleven 'negatives' for first and last visit. Three patients (1, 3, 19) show the extreme reverse situation with eleven 'plus'. Two intermediate cases are (i) patient 2 making a slight recovery and (ii) patient 8 showing no change. In the case of patient 2 and patient 8, further treatment is referred back to the medical expert.

10 Acknowledgement

We would like to acknowledge the contribution from Datin Dr. Hjh Aziah Mahyuddin and Dr. Azwayati Abas, The Respiratory Unit, Kuala Lumpur General Hospital, and Dr Hamidah Shaban, Selangor Medical Centre.

This research was funded under an IRPA grant from the Ministry of Science, Technology and the Environment and Universiti Teknologi Malaysia.

References:

[1] WHO: The Global Plan To Stop TB 2006-2015: Action For Life Towards A World Free Of Tuberculosis. Geneva; WHO, 2006.

[2] Middlemiss, H, "Radiology of the future in developing countries", British Journal of Radiology, 55, pp. 698-699, 1982.

[3] Moores, B.M., "Digital X-ray Imaging", IEE Proceedings, Vol. 134, part A, Number 2, Special Issues On Medical Imaging, 1987.

[4] Shaban, H, Medical Consultant for Respiratory Disease, Private Conversation, Institute of Respiratory Disease, Kuala Lumpur Hospital.

[5] Hill, Derek L G, Batchelor, Philipp G., Holden, Mark, and Hawkes, David. 2001. Medical Image Registration. Physics in Medicine and Biology. Vol. 46.

[6] Gonzalez, Rafael C., Woods, Richard E., Eddins, Steven L. 2004. Digital Image Processing Using MATLAB. Pearson Education, Inc.

[7] Barbara Zitova, Jan Flusser. 2003. Image Registration methods: a survey. Image and Vision Computing, vol. 21. 977-1000.

[8] Weisberg, S., Applied Linear Regression, New York, John Wiley, 1980.

[9] Fuller, W. A., Measurement Error Models, New York, John Wiley, 1987.

[10] Dolby, G. R., "The Ultrastructural Relation; A Synthesis of the Functional and Structural Relations", BIOMETRIKA, 63, pp. 30-50, 1976.

[11] Chang, Y. F., Rijal O. M. and Noor N. M., "Image Quality and Noise Evaluation", The Proceedings of the 7th International Symposium On Signal Processing and Its Applications (ISPAA 2003), Paris, France, 2003.

[12] Freund, R. J. and Wilson, W. J., Statistical Methods, Academic Press, 1997